Structure and stability of clusters of β-alanine in the gas phase: importance of the nature of intermolecular interactions.
Electronic Supplementary Information.

Dariusz Grzegorz Piekarski*[1] and Sergio Díaz-Tendero†[1,2]

[1]UAM, Departamento de Química, Módulo 13, Universidad Autónoma de Madrid, 28049 Madrid, Spain
[2]IFIMAC, Condensed Matter Physics Center (IFIMAC), 28049 Madrid, Spain

1 Thermostats

The input files to run molecular dynamic (MD) simulations with AMBER [1–4] were prepared using antechamber tools.[5] General Amber force field[6] were used with RESP charges[7] parametrized at the HF/6-31G* level of theory with the Gaussian09 program.[8] Energy minimization was carried out to remove the possible non-physical, accidental contacts after parameterizing. Then, different thermostats were tested in order to obtain physically meaningful results. For each thermostat the different parameters were converged at each stage of the MD simulation. First, the system was heated from T=0K to the target temperature and then propagated at this temperature. Three different thermostats were checked: Berendsen,[9] Andersen[10] and Langevin.[11] The best results were obtained using the Berendsen thermostat for the heating stage and Langevin thermostat for the production dynamics. However, for both thermostats the results were unsatisfying since we observed high oscillations in energy and temperature and a further extensive benchmark study for thermal equilibration was performed.

1.1 Berendsen thermostat convergence

Firstly, the conditions for the Berendsen thermostat were optimized. We performed an extensive study to choose the best set of parameters: time step, Δt (fs), and temperature coupling parameter, tautp (ps), by using the Berendsen thermostat for all clusters sizes consider in the manuscript. To

*Electronic address: dariusz.piekarski@uam.es
†Electronic address: sergio.diaztendero@uam.es

this, during the heating stage from T=0K to T=(50, 100, 150, 200, 250, 300)K we checked all combination for tautp=(0.5, 1, 1.5, 2, 2.5, 3, 5, 10, 15, 20, 25, 50, 100, 150, 200 and 250 picoseconds) and Δt=(0.0001, 0.0002, 0.0003, 0.0004, 0.0005, 0.0006, 0.0007, 0.0008, 0.0009 and 0.001 fs); over 5000 simulations. After analyzing the simulations we concluded that tautp=10 ps and Δt=0.2 fs are the most appropriate parameters, since the temperature is well equilibrated for each cluster size and for each excitation energy during the propagation stage. The plots for each cluster size and temperature with the chosen parameters are presented in Tables 1-4.

Quantity		Temperature					
		50K	100K	150K	200K	250K	300K
Parameter sets	tautp[ps]	10	10	10	10	10	10
	Δt[fs]	0.2	0.2	0.2	0.2	0.2	0.2
Energy curves		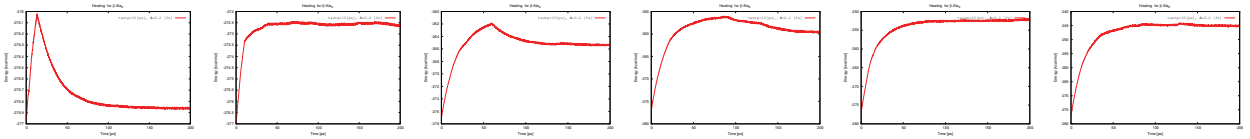					
Temperature curves		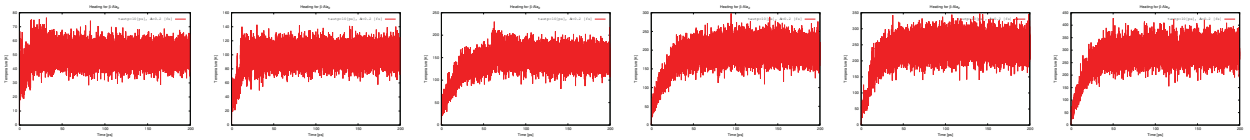					
Histogram full simulation		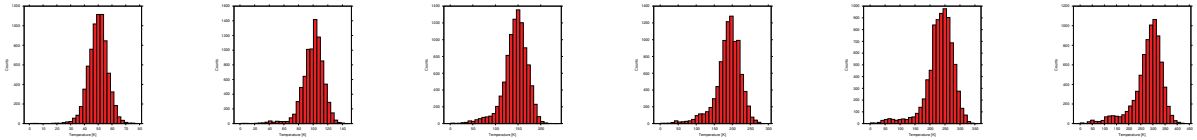					
Histogram last 100 ps		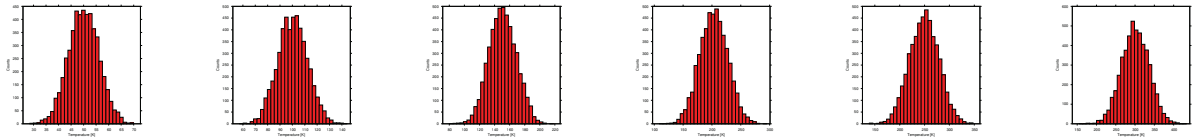					

Table 1: Parametrization using Berendsen thermostat for (β-Ala)$_2$

Quantity		Temperature					
		50K	100K	150K	200K	250K	300K
Parameter sets	tautp[ps]	10	10	10	10	10	10
	Δt[fs]	0.2	0.2	0.2	0.2	0.2	0.2
Energy curves		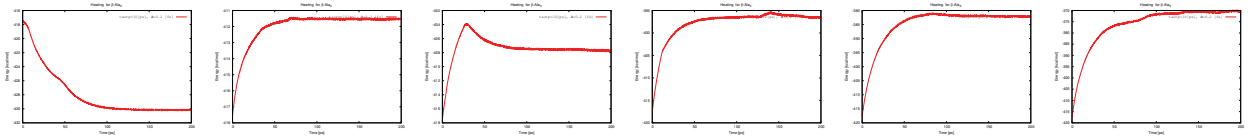					
Temperature curves		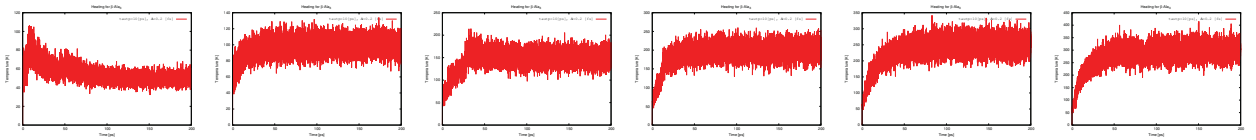					
Histogram full simulation		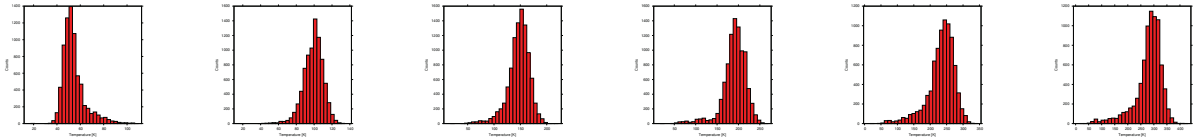					
Histogram last 100 ps		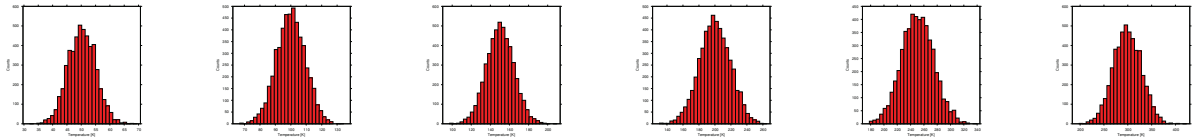					

Table 2: Parametrization using Berendsen thermostat for $(\beta\text{-Ala})_3$

Quantity		Temperature					
		50K	100K	150K	200K	250K	300K
Parameter sets	tautp[ps]	10	10	10	10	10	10
	Δt[fs]	0.2	0.2	0.2	0.2	0.2	0.2
Energy curves		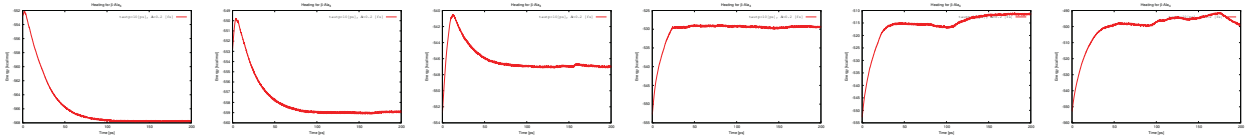					
Temperature curves		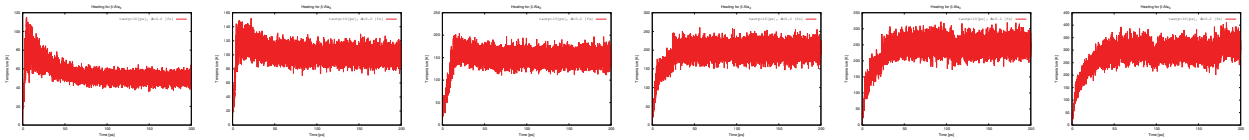					
Histogram full simulation		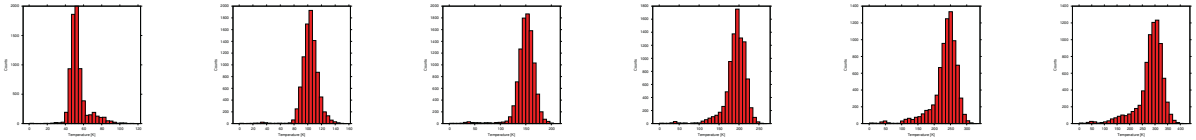					
Histogram last 100 ps		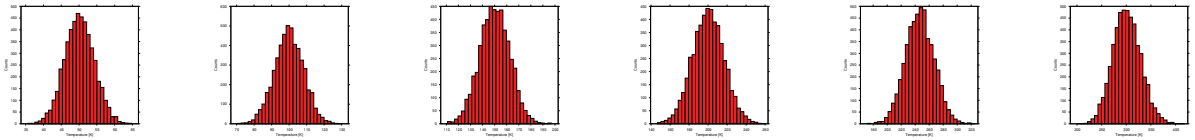					

Table 3: Parametrization using Berendsen thermostat for (β-Ala)$_4$

Quantity		Temperature					
		50K	100K	150K	200K	250K	300K
Parameter sets	tautp[ps]	10	10	10	10	10	10
	Δt[fs]	0.2	0.2	0.2	0.2	0.2	0.2
Energy curves		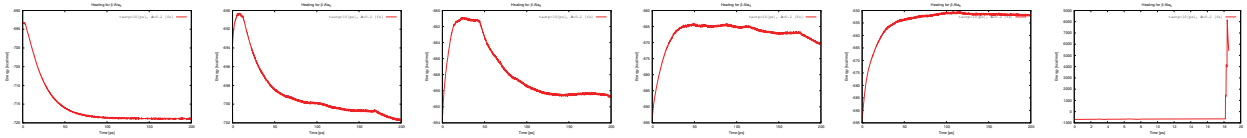					
Temperature curves		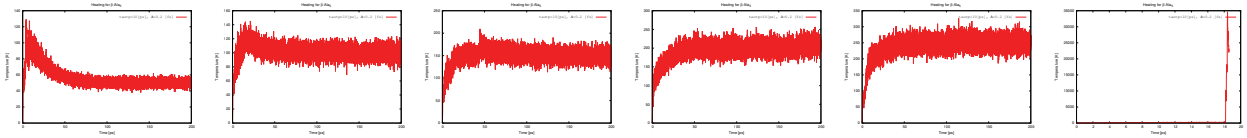					
Histogram full simulation		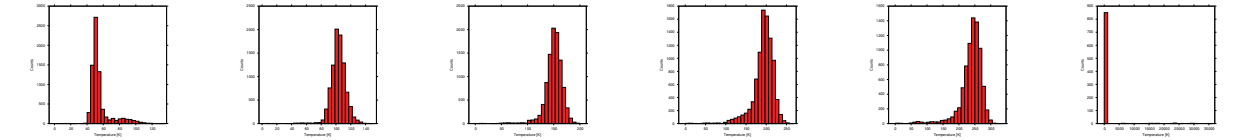					
Histogram last 100 ps		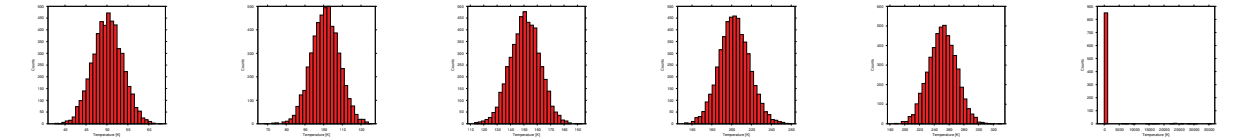					

Table 4: Parametrization using Berendsen thermostat for $(\beta\text{-Ala})_5$ For 300K cluster is not stable, it thermally breaks.

1.2 Langevin thermostat convergence

Secondly, we optimized the conditions for the Langevin thermostat. We performed an extensive study to choose the best set of parameters: time step, Δt (fs), and the collision frequency, γ (ps^{-1}). For the Langevin thermostat we considered the same cluster sizes and temperature values as for the Berendsen thermostat. Simulations were performed with γ=(1, 2, 3, 4, 5, 10, 20, 25, 50, 60, 70, 80, 90, 100 ps^{-1}) and Δt=(0.1, 0.2, ... 1.5, 2.0 fs). After these simulations we concluded that γ=5 ps^{-1} (weak coupling to approximate the micro-canonical ensemble, NVE) and Δt=0.2 fs are the most appropriate parameters, where the energy and the temperature are well equilibrated for each cluster size and for each temperature during the propagation stage. The plots for each cluster size and temperature with the chosen parameters are presented in Tables 5-8.

Quantity	Temperature					
	50K	100K	150K	200K	250K	300K
Energy curves	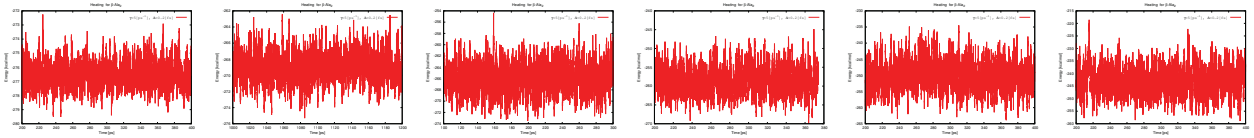					
Temperature curves	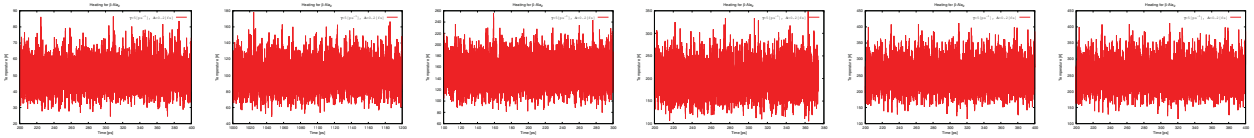					
Histogram full simulation	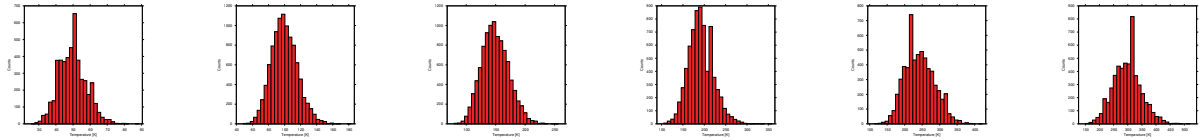					
Histogram last 100 ps	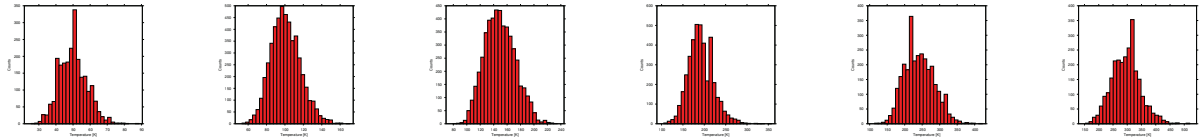					

Table 5: Parametrization using Langevin thermostat for (β-Ala)$_2$. Parameters for each temperature are: γ=5 ps^{-1} and Δt=0.2 fs.

Quantity	Temperature					
	50K	100K	150K	200K	250K	300K
Energy curves	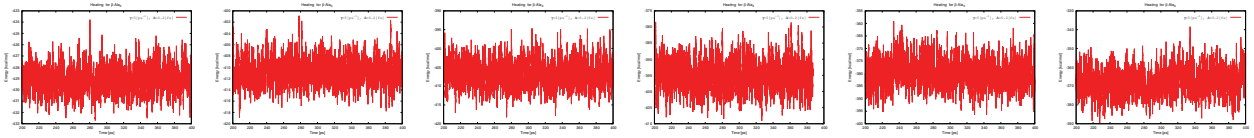					
Temperature curves	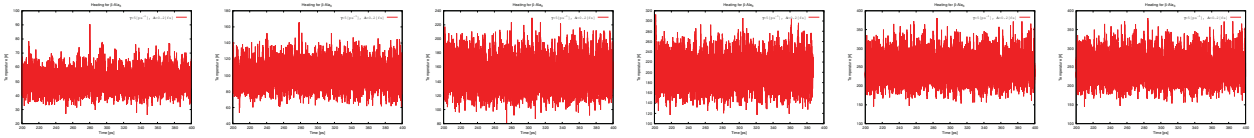					
Histogram full simulation	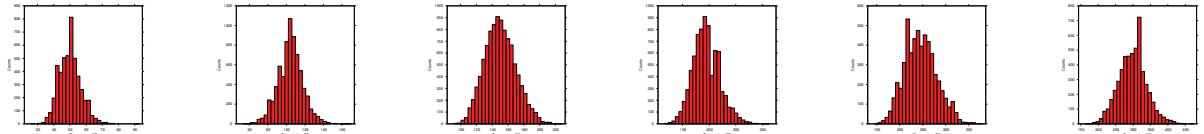					
Histogram last 100 ps	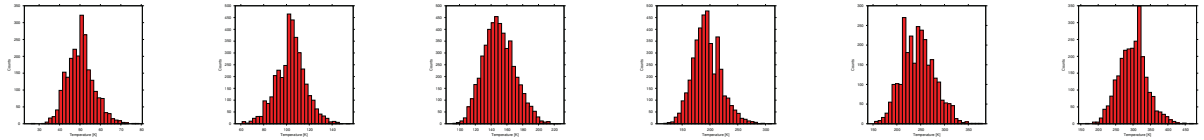					

Table 6: Parametrization using Langevin thermostat for (β-Ala)$_3$. Parameters for each temperature are: γ=5 ps^{-1} and Δt=0.2 fs.

Quantity	Temperature					
	50K	100K	150K	200K	250K	300K
Energy curves	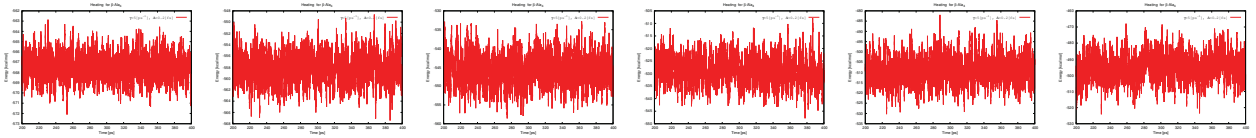					
Temperature curves	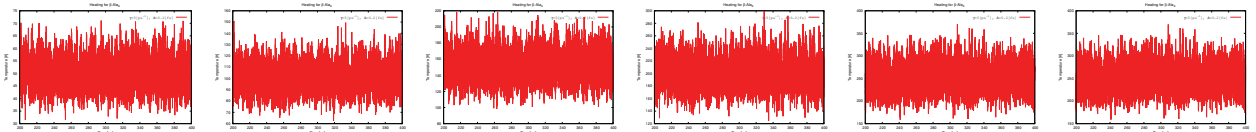					
Histogram full simulation	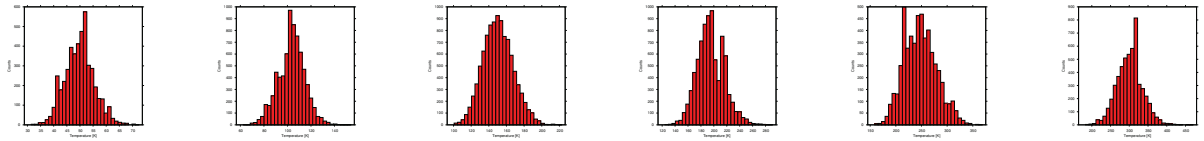					
Histogram last 100 ps	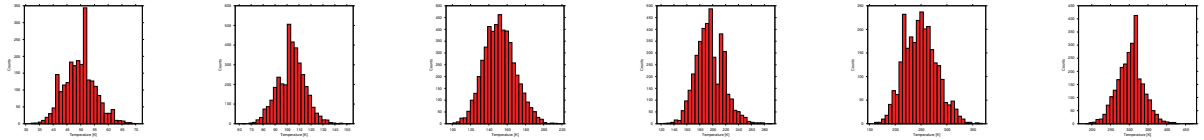					

Table 7: Parametrization using Langevin thermostat for (β-Ala)$_4$. Parameters for each temperature are: γ=5 ps^{-1} and Δt=0.2 fs.

Quantity	Temperature					
	50K	100K	150K	200K	250K	300K
Energy curves	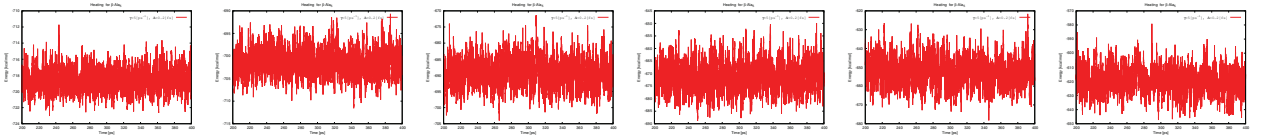					
Temperature curves	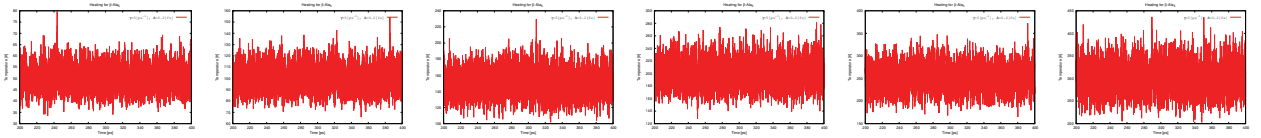					
Histogram full simulation	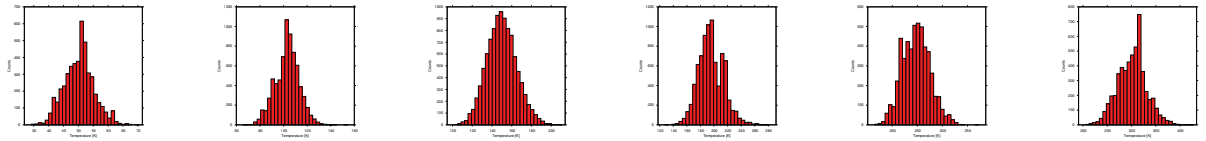					
Histogram last 100 ps	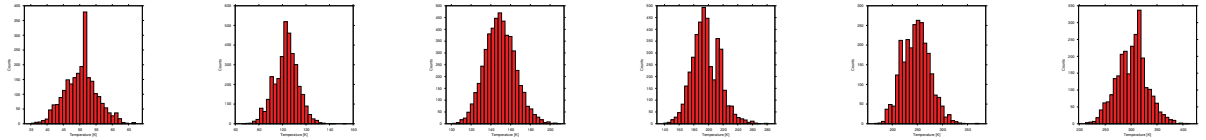					

Table 8: Parametrization using Langevin thermostat for (β-Ala)$_5$. Parameters for each temperature are: γ=5 ps^{-1} and Δt=0.2 fs.

1.3 Summary of the thermostats convergence

A large set of various parameters to run classical molecular dynamics simulations for both processes heating and propagation were considered. After the evaluation of these parameters we obtained the most stable ones for each temperature at the heating and production stages, using the Berendsen and Langevin thermostats, respectively. We checked that the total energy and temperature do not fluctuate as a function of time to be sure that system is well equilibrated. Some slight deviations in the temperature are observed due to the hydrogen bonds creation and annihilation, and due to van der Waals interactions.

2 Benchmarking

The benchmarking study has been carried out evaluating geometries, relative energies and bonding properties. Table 9 presents differences in the geometries obtained with the MP2 method and with each of the considered functionals: B3LYP, dispersion corrected B97D, M06 and its variation M06-2X and MPWB1K in combination with the 6-311++G(d,p) basis set. Benchmarking of some electron properties in the bond critical points (BCPs) of H bonds for the most stable dimer (2.1) are presented in Table 10. Figure 1 presents a general comparison of the relative energies of 19 conformers of dimers after geometry optimization with the MP2 method and all considered DFT functionals. Single point energies at the CCSD(T)/6-311++G(d,p) level of theory were obtained from geometries optimised at MP2 level of theory for the most stable 11 conformers. Figure 2 shows benchmarking of the relative energies computed with the DFT functionals and their correlation with the MP2 and CCSD(T) methods. Almost complete energetic similarity measured with the Pearson coefficient is found for the M06-2X functional in comparison with MP2 or CCSD(T).

Table 9: Root mean square deviations, $RMSD$ in Å, for the structures in $(\beta - ala)_2$ calculated for each considered functional with respect to the MP2 results. The biggest and the smallest values of $RMSD$ are highlighted in bold.

Conformer	B3LYP	B97D	M06	M06-2X	MPWB1K
2.1	0.08	**0.04**	0.04	0.05	0.05
2.2	0.13	0.11	0.17	0.13	0.13
2.3	0.10	0.09	0.12	0.13	0.13
2.4	0.14	0.11	0.25	0.29	0.25
2.5	0.28	0.26	0.31	**0.32**	0.31
2.6	0.12	0.12	0.35	0.25	0.30
2.7	0.19	0.18	0.34	0.14	0.25
2.8	0.08	0.12	0.12	0.10	0.08
2.9	**0.87**	**0.73**	**0.82**	0.16	**0.85**
2.10	0.16	0.05	0.09	0.06	0.07
2.11	0.45	0.05	0.17	0.09	0.08
2.12	0.54	0.10	0.13	0.12	0.13
2.13	0.56	0.11	0.08	0.06	0.14
2.14	0.07	0.05	**0.03**	0.04	**0.04**
2.15	0.22	0.16	0.11	0.17	0.25
2.16	0.10	0.09	0.08	0.17	0.09
2.17	**0.06**	0.05	**0.03**	**0.03**	**0.04**
2.18	0.70	0.11	0.19	0.10	0.10
2.19	0.44	0.21	0.06	0.22	0.46
Average	0.28	0.14	0.18	0.14	0.20

Table 10: Electron density and its Laplacian computed for the most stable conformer of $(\beta - ala)_2$ at the bond critical points BCP1 and BCP2 (see bonds labels in the main text).

	MP2	B3LYP	B97D	M06	M06-2X	MPWB1K
ρ (BCP1)	0.050	0.050	0.052	0.049	0.050	0.049
ρ (BCP2)	0.050	0.050	0.052	0.049	0.050	0.049
$\nabla^2\rho$ (BCP1)	0.100	0.100	0.093	0.108	0.100	0.104
$\nabla^2\rho$ (BCP2)	0.100	0.100	0.093	0.108	0.100	0.104

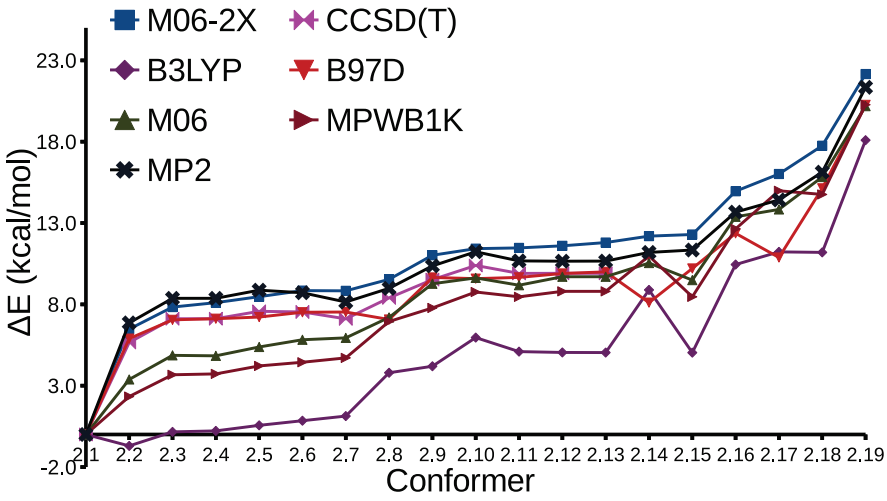

Figure 1: Benchmarking of 19 conformers of $(\beta - ala)_2$: relative stability between all conformers at the different levels of theory that we considered; Relative energies are given in kcal mol $^{-1}$ with respect to the most stable conformer.

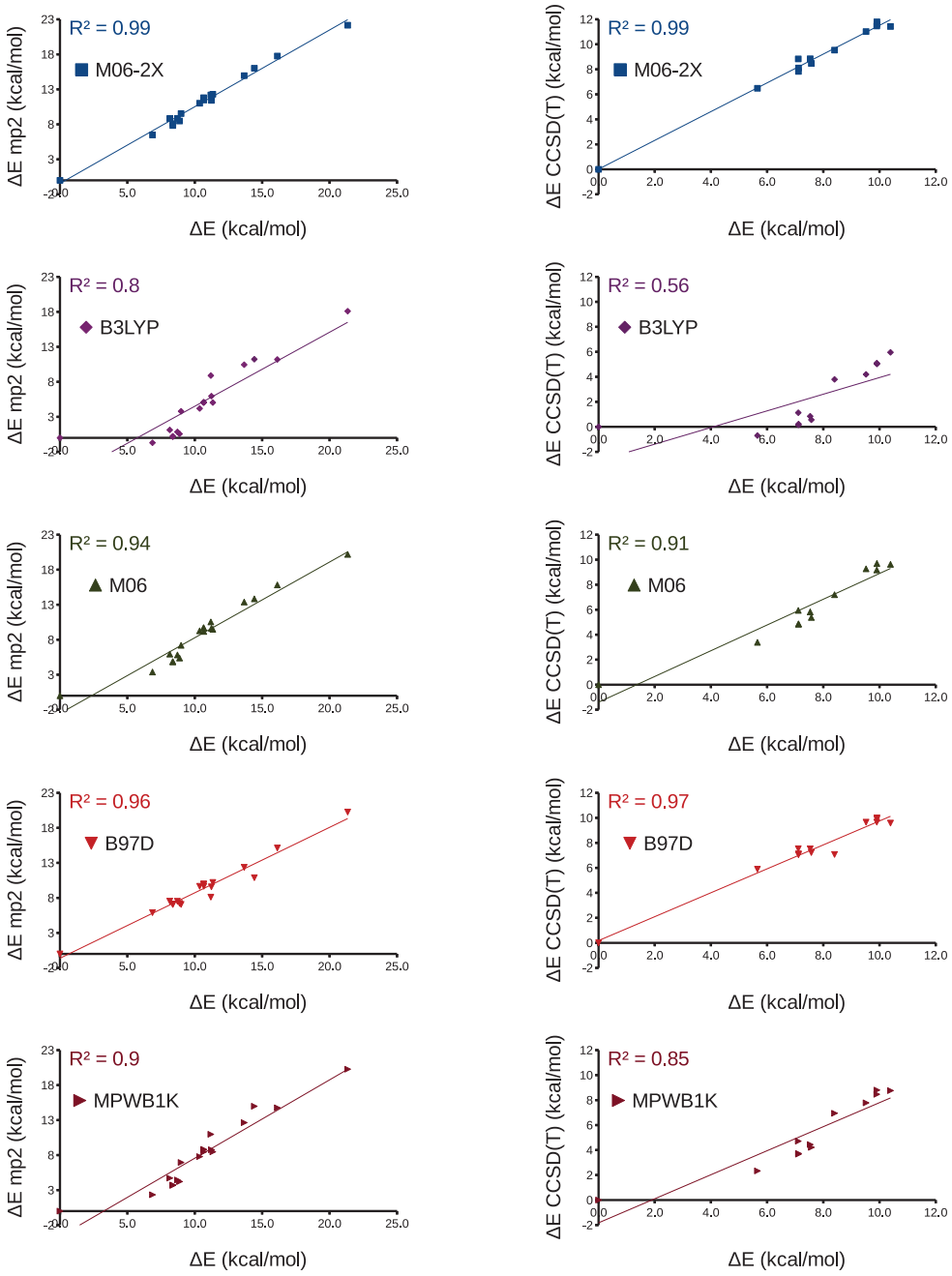

Figure 2: Benchmarking of 19 and 11 conformers of $(\beta-ala)_2$: correlations of the different functionals with the MP2 and CCSD(T) results, respectively. R is the Pearson correlation coefficient. Relative energies are given in kcal mol $^{-1}$ with respect to the most stable conformer (see all structures in the Figure 4.

3 Isomers

Using the computational strategy described in the main manuscript and employing the M06-2X functional with the 6-311++G(d,p) basis set we evaluated the relative stability of numerous isomers (m) of different cluster sizes (n). We use the nomenclature (n,m), e.g. conformer 3.9 is the ninth conformer of a cluster with three beta-alanine residues. A complete study of the isomers of neutral β-alanine molecules is presented in Figures 3-10. We present the optimized geometries, stabilized mainly through hydrogen bonds, and their relative energies. The monomers were obtained after reoptimization of geometries taken from a previous study. [12]

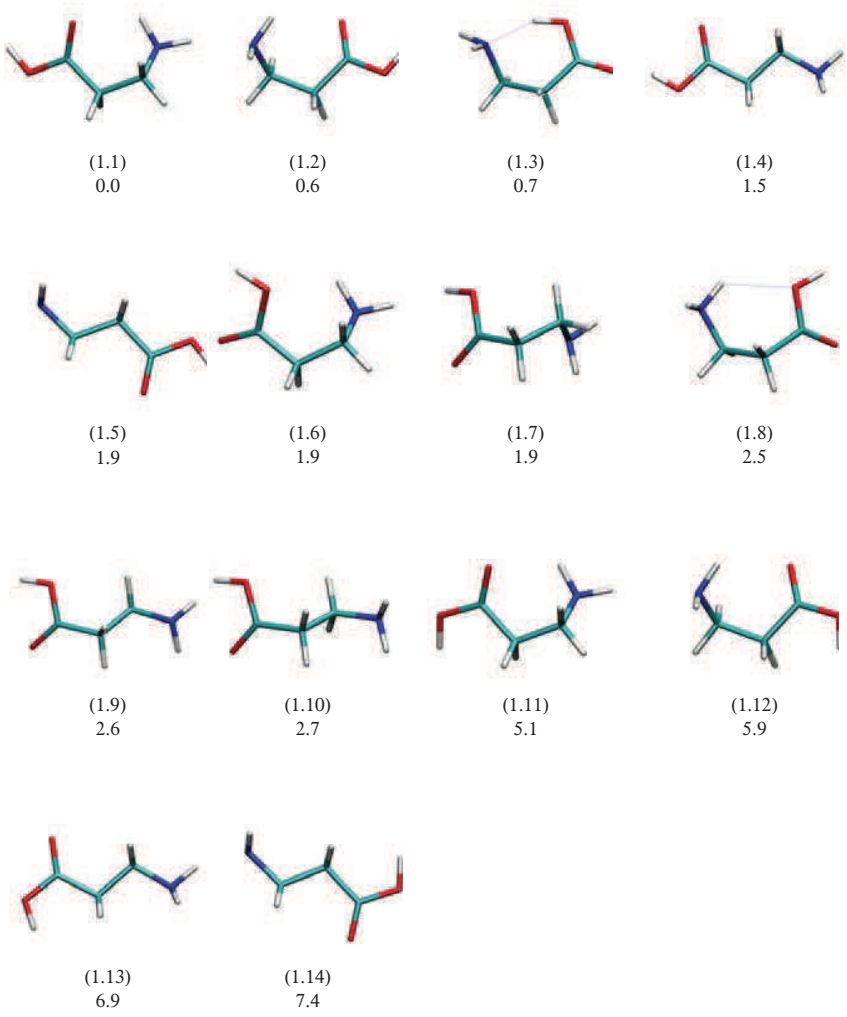

Figure 3: Optimized geometries of neutral monomers (1.1-1.14) of β-alanine at the DFT-M06-2X/6-311++G(d,p) level of theory. Relative energies with respect to the most stable neutral monomer (1.1) in kcal mol^{-1}.

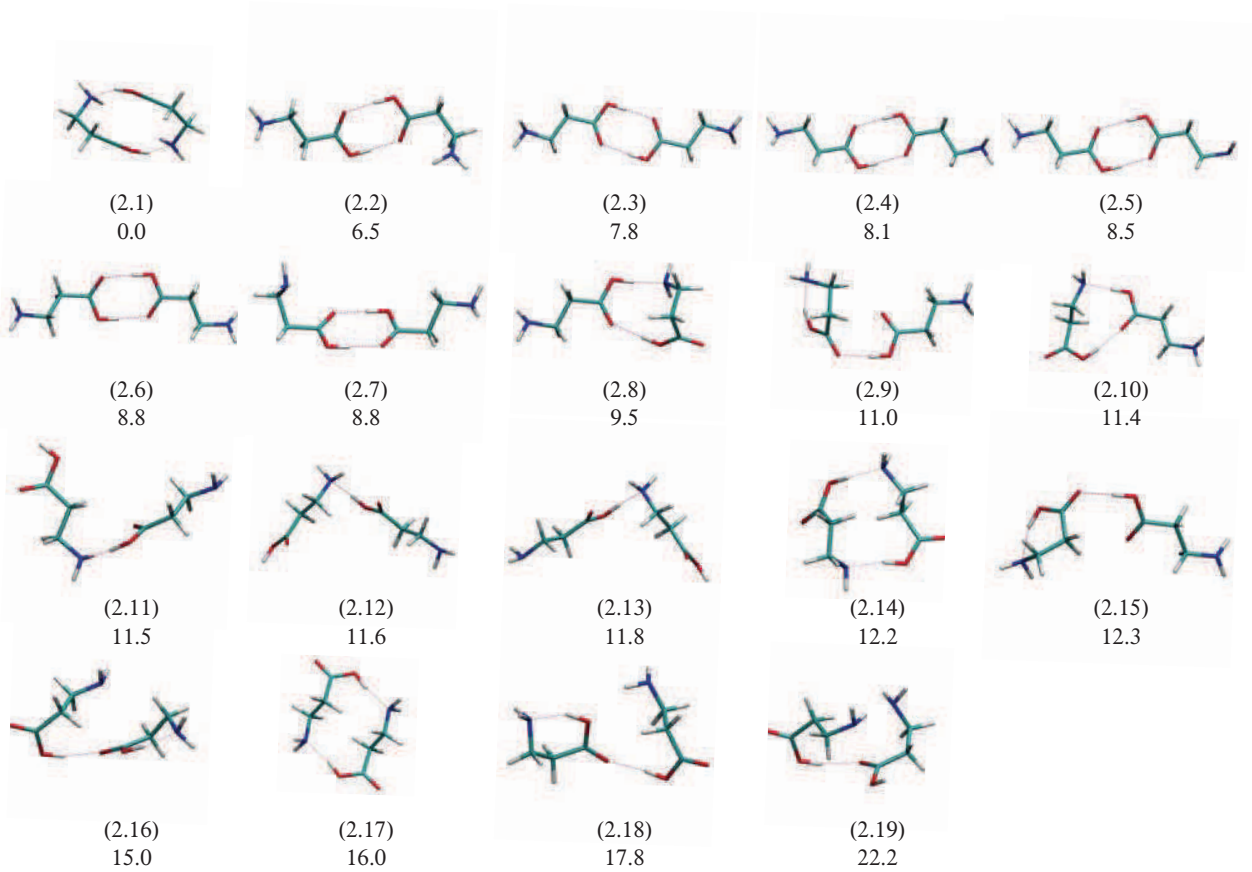

Figure 4: Optimized geometries of neutral dimers (2.1-2.19) of β-alanine at the DFT-M06-2X/6-311++G(d,p) level of theory. Relative energies with respect to the most stable neutral dimer (2.1) in kcal mol^{-1}. Dashed lines shows hydrogen (H) bonds with donor (D)-acceptor (A) atoms with the cut-off distance ≤ 3.2 and D-H-A angle ≤ 50 degree.[13] The colors of hydrogen bond: red, blue and turquoise underline the donor atom: oxygen, nitrogen and carbon, respectively.

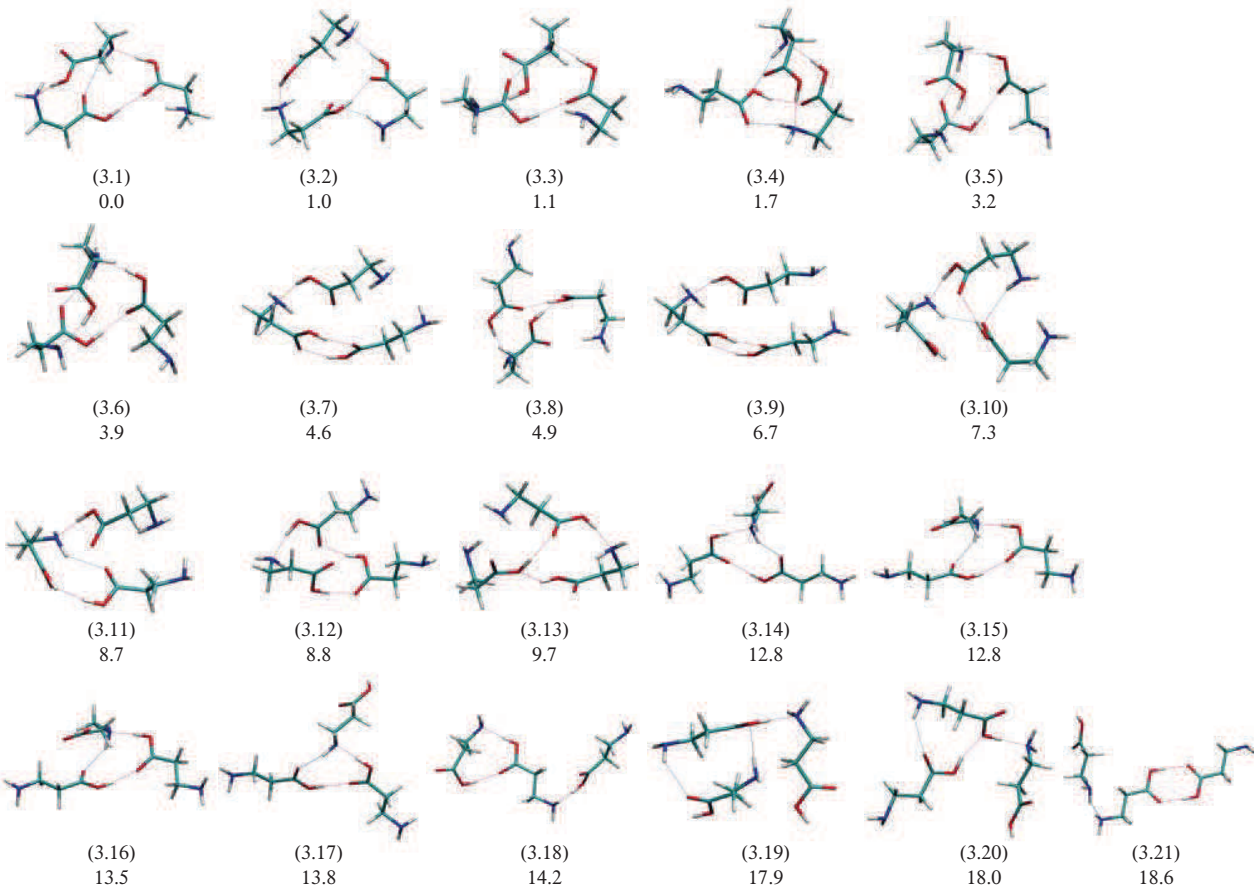

Figure 5: Optimized geometries of neutral trimers (3.1-3.21) of β-alanine at the DFT-M06-2X/6-311++G(d,p) level of theory. Relative energies with respect to the most stable neutral trimer (3.1) in kcal mol^{-1}. Dashed lines shows hydrogen (H) bonds with donor (D)-acceptor (A) atoms with the cut-off distance ≤ 3.2 and D-H-A angle ≤ 50 degree.[13] The colors of hydrogen bond: red, blue and turquoise underline the donor atom: oxygen, nitrogen and carbon, respectively.

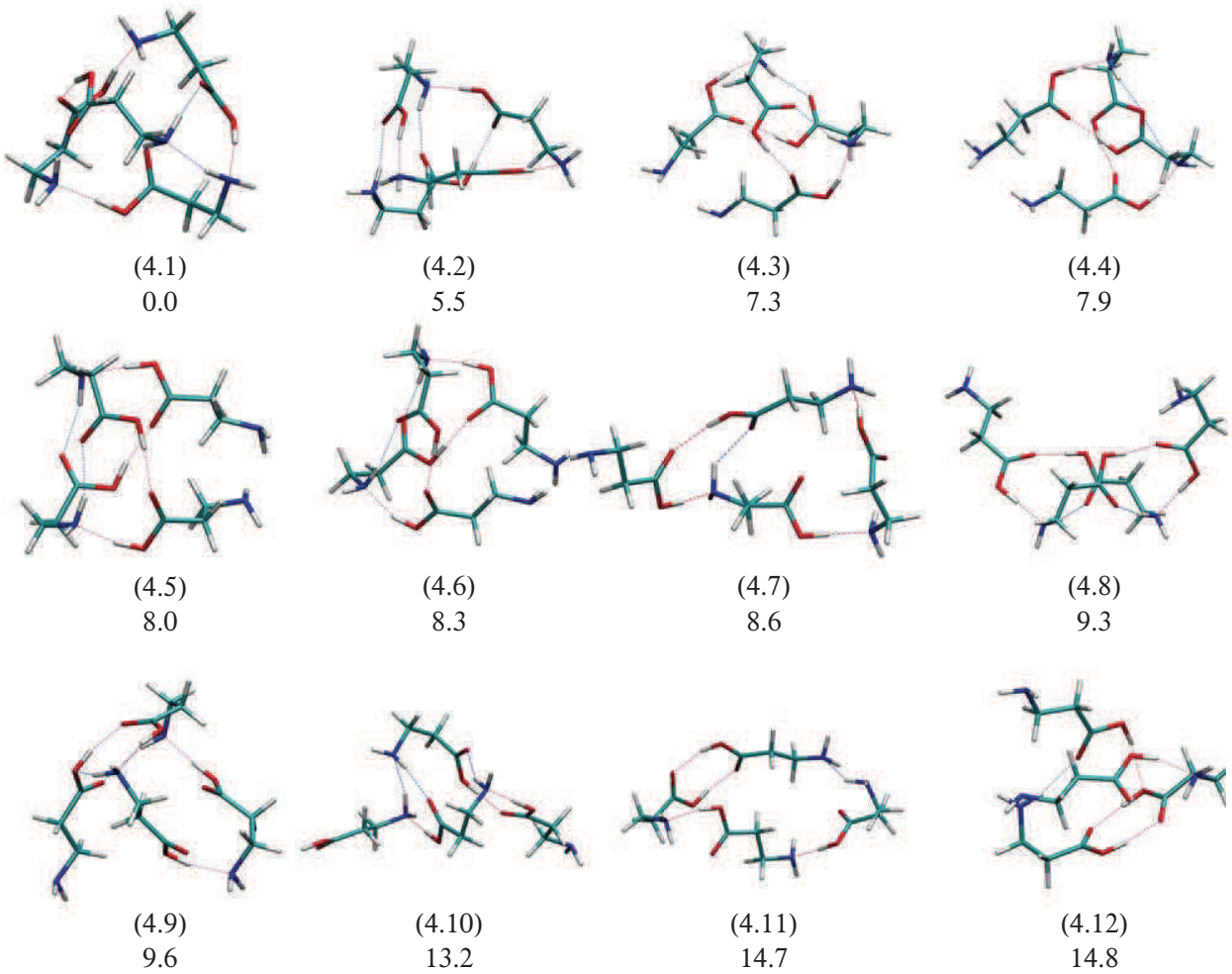

Figure 6: Optimized geometries of neutral tetramers (4.1-4.12) of β-alanine at the DFT-M06-2X/6-311++G(d,p) level of theory. Relative energies with respect to the most stable neutral tetramer (4.1) in kcal mol^{-1}. Dashed lines shows hydrogen (H) bonds with donor (D)-acceptor (A) atoms with the cut-off distance ≤ 3.2 and D-H-A angle ≤ 50 degree.[13] The colors of hydrogen bond: red, blue and turquoise underline the donor atom: oxygen, nitrogen and carbon, respectively.

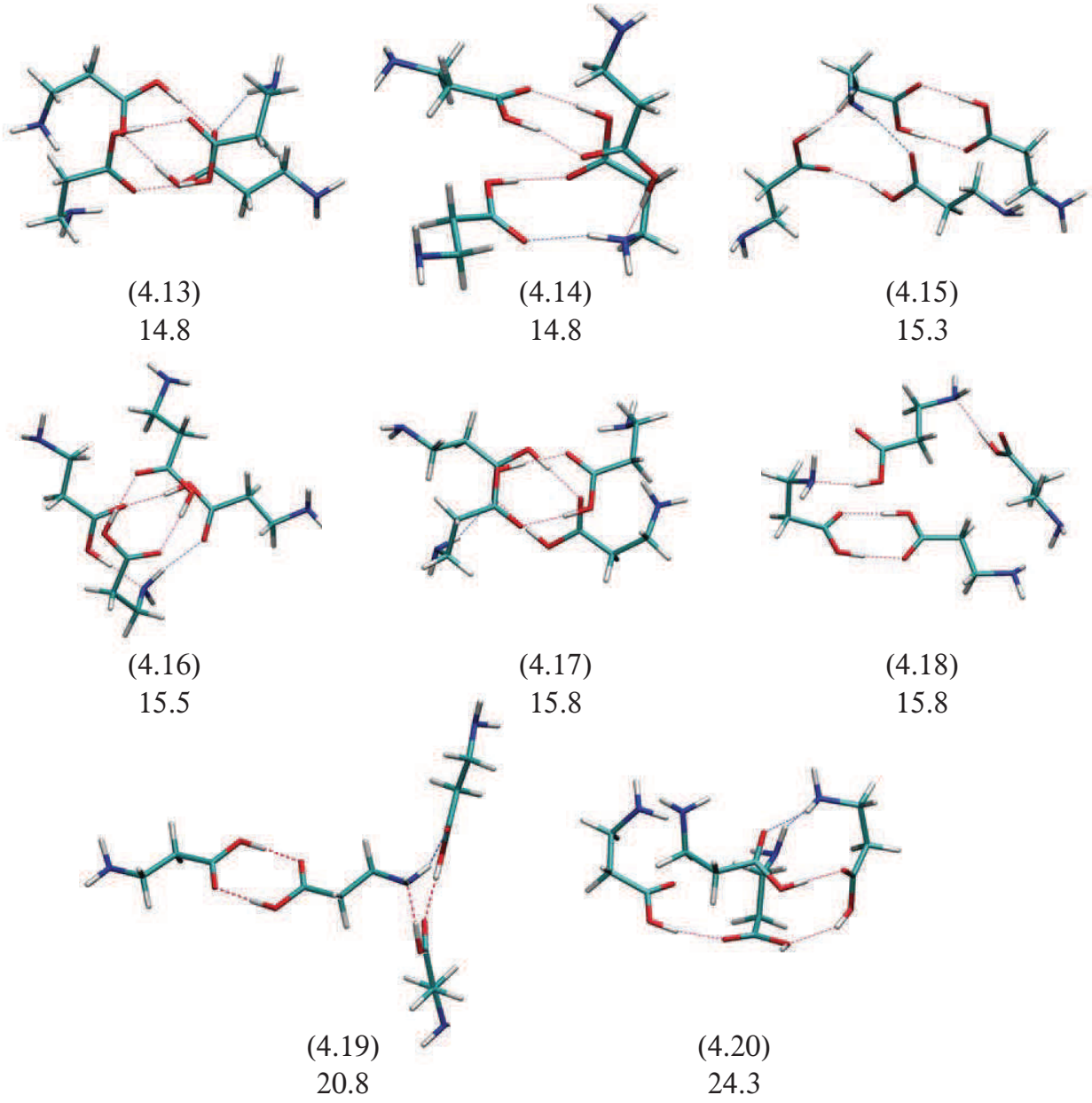

Figure 7: Optimized geometries of neutral tetramers (4.13-4.20) of β-alanine at the DFT-M06-2X/6-311++G(d,p) level of theory. Relative energies with respect to the most stable neutral tetramer (4.1) in kcal mol^{-1}. Dashed lines shows hydrogen (H) bonds with donor (D)-acceptor (A) atoms with the cut-off distance $\leq$ 3.2 and D-H-A angle $\leq$ 50 degree.[13] The colors of hydrogen bond: red, blue and turquoise underline the donor atom: oxygen, nitrogen and carbon, respectively.

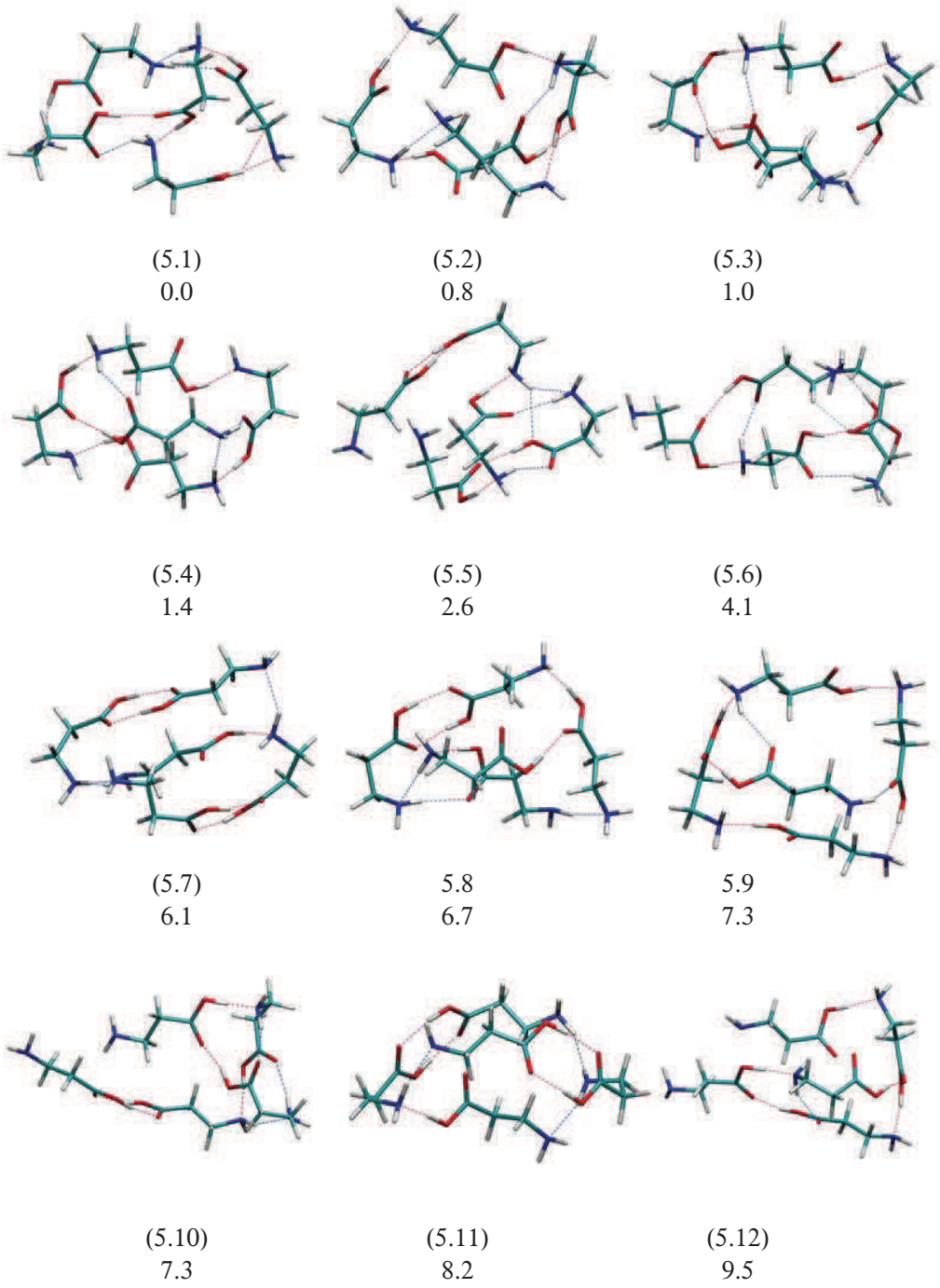

Figure 8: Optimized geometries of neutral pentamers (5.1-5.12) of β-alanine at the DFT-M06-2X/6-311++G(d,p) level of theory. Relative energies with respect to the most stable neutral tetramer (5.1) in kcal mol^{-1}. Dashed lines shows hydrogen (H) bonds with donor (D)-acceptor (A) atoms with the cut-off distance $\leq$ 3.2 and D-H-A angle $\leq$ 50 degree.[13] The colors of hydrogen bond: red, blue and turquoise underline the donor atom: oxygen, nitrogen and carbon, respectively.

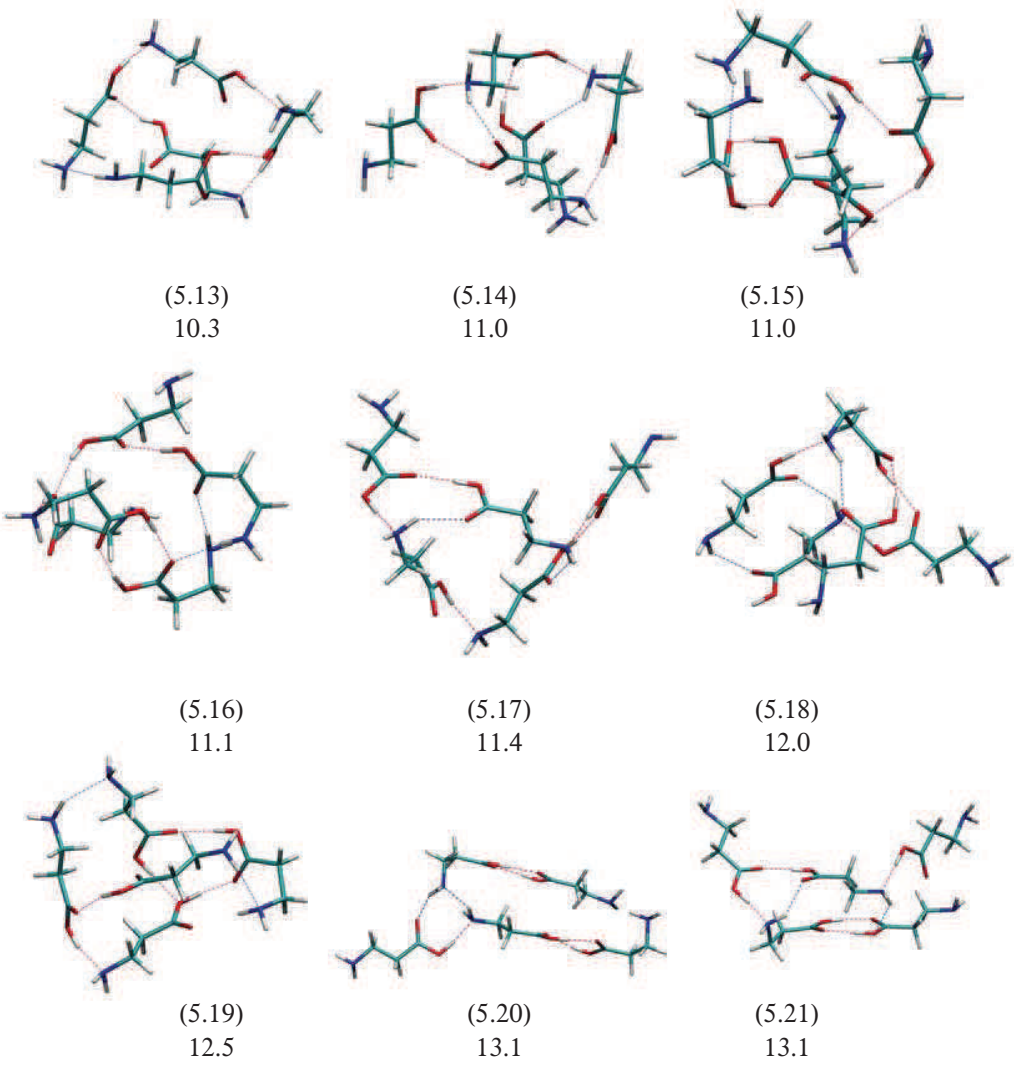

Figure 9: Optimized geometries of neutral pentamers (5.13-5.21) of β-alanine at the DFT-M06-2X/6-311++G(d,p) level of theory. Relative energies with respect to the most stable neutral tetramer (5.1) in kcal mol^{-1}. Dashed lines shows hydrogen (H) bonds with donor (D)-acceptor (A) atoms with the cut-off distance ≤ 3.2 and D-H-A angle ≤ 50 degree.[13] The colors of hydrogen bond: red, blue and turquoise underline the donor atom: oxygen, nitrogen and carbon, respectively.

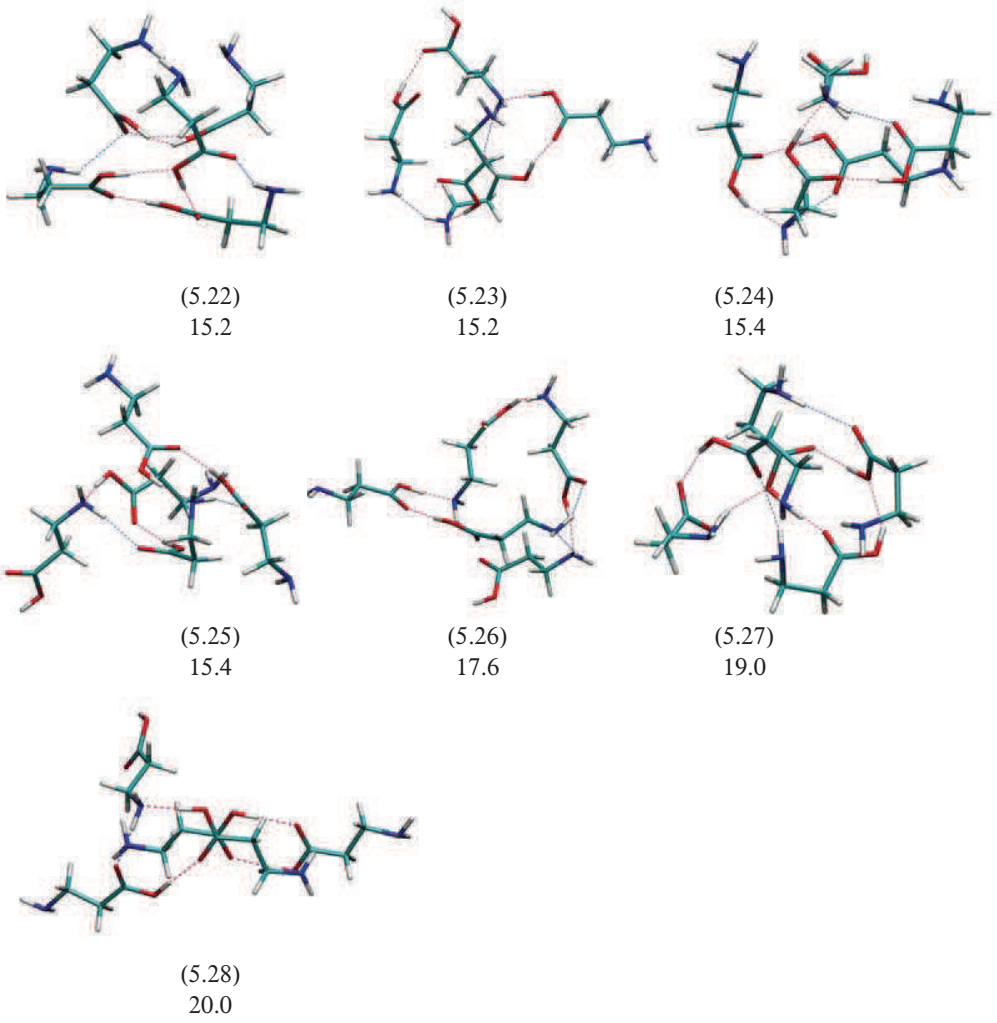

Figure 10: Optimized geometries of neutral pentamers (5.22-5.28) of β-alanine at the DFT-M06-2X/6-311++G(d,p) level of theory. Relative energies with respect to the most stable neutral tetramer (5.1) in kcal mol^{-1}. Dashed lines shows hydrogen (H) bonds with donor (D)-acceptor (A) atoms with the cut-off distance $\leq$ 3.2 and D-H-A angle $\leq$ 50 degree.[13] The colors of hydrogen bond: red, blue and turquoise underline the donor atom: oxygen, nitrogen and carbon, respectively.

Finally, we present a thorough study based on wave function analysis techniques for the most stable conformer of each cluster size. We focused on the estimated stabilization energies for all evaluated hydrogen bonds including a detailed analysis of the type of the donor hydrogen atom, acceptor hydrogen atom, acceptor and donor orbital energy differences and Fock-diagonal NBO Fock matrix elements.

Table 11: Estimated stabilization energy ($\Delta E_{ij}^{(2)}$) (in kcal mol^{-1}) of all the interaction between atoms involved in the hydrogen bonds (HBs) for the most stable dimer. Acceptor and donor orbital energy differences ($\epsilon_j^{(NL)} - \epsilon_i^{(L)}$) in a.u. and off-diagonal NBO Fock matrix elements (F_{ij}) in a.u. are also presented.

DIMER (β-ala)$_2$

HBs index	Donor NBO (i)					Acceptor NBO (j)					$\Delta E_{ij}^{(2)}$	$\epsilon_j^{(NL)} - \epsilon_i^{(L)}$	F_{ij}
1	BD	C	2	N	3	BD*	O	18	H	22	0.28	1.25	0.017
	BD	N	3	H	7	BD*	O	18	H	22	0.28	1.15	0.016
	BD	N	3	H	8	BD*	O	18	H	22	1.62	1.15	0.039
	CR	N	3	-	-	BD*	O	18	H	22	0.38	15.02	0.069
	LP	N	3	-	-	BD*	O	18	H	22	34.94	0.86	0.155
	BD	O	18	H	22	RY*	N	3	-	-	0.07	1.56	0.01
	BD	O	18	H	22	BD*	C	2	N	3	0.07	1.22	0.008
	BD	O	18	H	22	BD*	N	3	H	7	0.15	1.32	0.013
	BD	O	18	H	22	BD*	N	3	H	8	0.06	1.33	0.008
2	BD	O	5	H	9	RY*	N	16	-	-	0.07	1.56	0.01
	BD	O	5	H	9	BD*	C	15	N	16	0.07	1.22	0.008
	BD	O	5	H	9	BD*	N	16	H	20	0.15	1.32	0.013
	BD	O	5	H	9	BD*	N	16	H	21	0.06	1.33	0.008
	BD	C	15	N	16	BD*	O	5	H	9	0.27	1.25	0.017
	BD	N	16	H	20	BD*	O	5	H	9	0.28	1.15	0.016
	BD	N	16	H	21	BD*	O	5	H	9	1.62	1.15	0.039
	CR	N	16	-	-	BD*	O	5	H	9	0.38	15.02	0.069
	LP	N	16	-	-	BD*	O	5	H	9	34.94	0.86	0.155

Table 12: See caption of 11.

TRIMER (β-ala)$_3$

HBs index	Donor NBO (i)					Acceptor NBO (j)					$\Delta E_{ij}^{(2)}$	$\epsilon_j^{(NL)} - \epsilon_i^{(L)}$	F_{ij}
1	BD	O	3	H	4	RY*	N	37	-	-	0.08	1.61	0.010
	BD	O	3	H	4	RY*	N	37	-	-	0.07	1.86	0.011
	BD	O	3	H	4	RY*	N	37	-	-	0.06	2.35	0.011
	BD	O	3	H	4	BD*	C	34	N	37	0.08	1.18	0.009
	BD	O	3	H	4	BD*	N	37	H	39	0.07	1.30	0.009
	BD*	O	3	H	4	RY*	N	37	-	-	1.07	0.02	0.014
	BD*	O	3	H	4	RY*	N	37	-	-	0.17	0.35	0.025
	BD	C	34	N	37	BD*	O	3	H	4	1.66	1.19	0.041
	BD	N	37	H	38	BD*	O	3	H	4	1.97	1.10	0.043
	BD	N	37	H	39	BD*	O	3	H	4	1.88	1.10	0.042
	CR	N	37	-	-	BD*	O	3	H	4	1.55	14.97	0.141
	LP	N	37	-	-	BD*	O	3	H	4	80.1	0.79	0.226
2	BD	C	15	O	18	BD*	N	37	H	39	0.31	0.96	0.015
	LP	O	18	-	-	BD*	N	37	H	39	2.53	1.31	0.051
	LP	O	18	-	-	BD*	N	37	H	39	1.48	0.85	0.033
	BD*	C	15	O	18	BD*	N	37	H	39	0.11	0.45	0.018
	BD	N	37	H	39	BD*	C	15	O	18	0.07	0.77	0.007
3	BD	C	21	N	24	BD*	O	29	H	30	0.15	1.26	0.012
	BD	N	24	H	25	BD*	O	29	H	30	0.14	1.16	0.012
	BD	N	24	H	26	BD*	O	29	H	30	1.45	1.15	0.037
	CR	N	24	-	-	BD*	O	29	H	30	0.23	15.02	0.054
	LP	N	24	-	-	BD*	O	29	H	30	26.84	0.86	0.136
	BD	O	29	H	30	RY*	N	24	-	-	0.07	1.78	0.010
	BD	O	29	H	30	BD*	C	21	N	24	0.07	1.23	0.008
	BD	O	29	H	30	BD*	N	24	H	25	0.18	1.33	0.014
	BD	O	29	H	30	BD*	N	24	H	26	0.1	1.33	0.010
4	BD	C	2	O	5	BD*	O	16	H	17	0.27	1.65	0.019
	BD	C	2	O	5	BD*	O	16	H	17	1.50	0.95	0.034
	CR	O	5	-	-	BD*	O	16	H	17	0.19	19.85	0.056
	LP	O	5	-	-	BD*	O	16	H	17	15.13	1.28	0.124
	LP	O	5	-	-	BD*	O	16	H	17	3.67	0.85	0.051
	BD*	C	2	O	5	BD*	O	16	H	17	0.66	0.43	0.038
	BD	O	16	H	17	RY*	O	5	-	-	0.12	1.63	0.013
	BD	O	16	H	17	RY*	O	5	-	-	0.36	2.54	0.027
	BD	O	16	H	17	BD*	C	2	O	5	0.34	1.51	0.020
	BD	O	16	H	17	BD*	C	2	O	5	0.25	0.9	0.014

Table 13: See caption of 11.

TETRAMER (β-ala)$_4$

HBs index	Donor NBO (i)					Acceptor NBO (j)					$\Delta E_{ij}^{(2)}$	$\epsilon_j^{(NL)} - \epsilon_i^{(L)}$	F_{ij}
1	BD	O	3	H	4	RY*	N	37	-	-	0.10	2.56	0.014
	BD	O	3	H	4	BD*	C	34	N	37	0.09	1.19	0.009
	BD	O	3	H	4	BD*	N	37	H	38	0.08	1.27	0.009
	BD*	O	3	H	4	RY*	N	37	-	-	0.09	0.40	0.020
	BD	C	34	N	37	BD*	O	3	H	4	1.22	1.20	0.035
	BD	N	37	H	38	BD*	O	3	H	4	1.53	1.10	0.038
	BD	N	37	H	39	BD*	O	3	H	4	2.06	1.10	0.044
	CR	N	37	-	-	BD*	O	3	H	4	1.33	14.97	0.131
	LP	N	37	-	-	BD*	O	3	H	4	71.11	0.80	0.214
2	BD	C	2	O	5	BD*	O	16	H	17	0.44	1.64	0.024
	BD	C	2	O	5	BD*	O	16	H	17	2.28	0.95	0.042
	CR	O	5	-	-	BD*	O	16	H	17	0.26	19.84	0.065
	LP	O	5	-	-	BD*	O	16	H	17	13.83	1.26	0.118
	LP	O	5	-	-	BD*	O	16	H	17	9.78	0.85	0.083
	BD*	C	2	O	5	BD*	O	16	H	17	1.06	0.42	0.047
	BD	O	16	H	17	RY*	O	5	-	-	0.05	2.58	0.011
	BD	O	16	H	17	BD*	C	2	O	5	0.19	1.50	0.015
	BD	O	16	H	17	BD*	C	2	O	5	0.44	0.91	0.019
3	BD	N	11	H	13	RY*	O	18	-	-	0.10	1.98	0.013
	BD	N	11	H	13	BD*	C	15	O	18	0.13	0.79	0.010
	BD	C	15	O	18	BD*	N	11	H	13	0.47	1.00	0.019
	LP	O	18	-	-	BD*	N	11	H	13	2.46	1.31	0.051
	LP	O	18	-	-	BD*	N	11	H	13	2.60	0.86	0.043
	BD*	C	15	O	18	BD*	N	11	H	13	0.20	0.44	0.024
4	BD	N	24	H	26	RY*	O	44	-	-	0.10	1.35	0.010
	BD	N	24	H	26	RY*	O	44	-	-	0.08	1.64	0.010
	BD	N	24	H	26	BD*	C	41	O	44	0.10	0.74	0.008
	BD	C	41	O	44	BD*	N	24	H	26	0.96	0.96	0.027
	LP	O	44	-	-	BD*	N	24	H	26	0.39	1.31	0.020
	LP	O	44	-	-	BD*	N	24	H	26	0.32	0.85	0.015
	BD*	C	41	O	44	BD*	N	24	H	26	0.11	0.45	0.018
5	BD	N	24	H	25	RY*	O	31	-	-	0.06	1.74	0.010
	BD	N	24	H	25	RY*	O	31	-	-	0.15	2.10	0.016
	BD	N	24	H	25	BD*	C	28	O	31	0.05	1.37	0.007
	BD	N	24	H	25	BD*	C	28	O	31	0.19	0.75	0.011
	BD	C	28	O	31	BD*	N	24	H	25	0.38	0.98	0.017
	LP	O	31	-	-	BD*	N	24	H	25	2.15	1.32	0.048
	LP	O	31	-	-	BD*	N	24	H	25	0.89	0.87	0.025
	BD*	C	28	O	31	BD*	N	24	H	25	0.16	0.46	0.021
6	BD	N	24	H	25	BD*	N	50	H	52	0.43	1.19	0.020
	BD	N	24	H	26	BD*	N	50	H	52	0.35	1.19	0.018
	LP	N	24	-	-	BD*	N	50	H	52	11.15	0.89	0.090
	BD	N	50	H	-	RY*	N	24	-	-	0.07	1.53	0.009
	BD	N	50	H	52	RY*	N	24	-	-	0.18	1.95	0.017
	BD	N	50	H	52	BD*	C	21	N	24	0.29	1.15	0.016

Table 13: See caption of 11.

TETRAMER (β-ala)$_4$

HBs index	Donor NBO (i)					Acceptor NBO (j)					$\Delta E_{ij}^{(2)}$	$\epsilon_j^{(NL)} - \epsilon_i^{(L)}$	F_{ij}
7	BD	O	29	H	30	RY*	N	50	-	-	0.06	1.71	0.009
	BD	O	29	H	30	RY*	N	50	-	-	0.08	2.63	0.013
	BD	O	29	H	30	BD*	C	47	N	50	0.06	1.21	0.008
	BD	O	29	H	30	BD*	N	50	H	51	0.08	1.29	0.009
	BD*	O	29	H	30	RY*	N	50	-	-	0.07	0.46	0.022
	BD*	O	29	H	30	RY*	N	50	-	-	0.07	0.33	0.018
	BD*	O	29	H	30	RY*	N	50	-	-	0.09	0.26	0.018
	BD*	O	29	H	30	BD*	N	50	H	51	0.09	0.05	0.008
	BD	C	47	N	50	BD*	O	29	H	30	0.75	1.23	0.028
	BD	N	50	H	51	BD*	O	29	H	30	0.85	1.12	0.028
	BD	N	50	H	52	BD*	O	29	H	30	1.92	1.13	0.043
	CR	N	50	-	-	BD*	O	29	H	30	0.83	14.99	0.102
	LP	N	50	-	-	BD*	O	29	H	30	53.91	0.82	0.189
8	BD	C	8	N	11	BD*	O	42	H	43	0.90	1.21	0.030
	BD	N	11	H	12	BD*	O	42	H	43	1.26	1.11	0.034
	BD	N	11	H	13	BD*	O	42	H	43	1.96	1.11	0.043
	CR	N	11	-	-	BD*	O	42	H	43	1.07	14.98	0.117
	LP	N	11	-	-	BD*	O	42	H	43	64.44	0.81	0.205
	BD	O	42	H	43	RY*	N	11	-	-	0.11	1.77	0.013
	BD	O	42	H	43	RY*	N	11	-	-	0.09	2.57	0.013
	BD	O	42	H	43	BD*	C	8	N	11	0.12	1.21	0.011
	BD*	O	42	H	43	RY*	N	11	-	-	0.06	0.17	0.011
	BD*	O	42	H	43	RY*	N	11	-	-	0.47	0.13	0.027
	BD*	O	42	H	43	BD*	N	11	H	12	0.06	0.07	0.007

Table 14: See caption of 11.

PENTAMER (β-ala)$_5$

HBs index	Donor NBO (i)					Acceptor NBO (j)					$\Delta E_{ij}^{(2)}$	$\epsilon_j^{(NL)} - \epsilon_i^{(L)}$	F_{ij}
1	BD	O	16	H	17	RY*	N	50	-	-	0.05	1.72	0.008
	BD	O	16	H	17	RY*	N	50	-	-	0.08	2.31	0.012
	BD	O	16	H	17	BD*	N	50	H	51	0.09	1.30	0.010
	BD*	O	16	H	17	RY*	N	50	-	-	0.14	0.38	0.029
	BD*	O	16	H	17	RY*	N	50	-	-	0.07	0.24	0.016
	BD*	O	16	H	17	BD*	N	50	H	51	0.08	0.05	0.008
	BD	C	47	N	50	BD*	O	16	H	17	0.54	1.24	0.024
	BD	N	50	H	51	BD*	O	16	H	17	0.59	1.13	0.024
	BD	N	50	H	52	BD*	O	16	H	17	1.38	1.14	0.036
	CR	N	50	-	-	BD*	O	16	H	17	0.59	15.00	0.086
	LP	N	50	-	-	BD*	O	16	H	17	44.90	0.84	0.174
2	BD	N	50	H	52	RY*	N	63	-	-	0.11	1.72	0.012
	BD	N	50	H	52	RY*	N	63	-	-	0.10	2.44	0.014
	BD	N	50	H	52	BD*	C	60	N	63	0.11	1.13	0.010
	BD	N	63	H	64	BD*	N	50	H	52	0.61	1.18	0.024
	LP	N	63	-	-	BD*	N	50	H	52	10.35	0.89	0.086

Table 14: See caption of 11.

PENTAMER (β-ala)$_5$

HBs index	Donor NBO (i)					Acceptor NBO (j)					$\Delta E_{ij}^{(2)}$	$\epsilon_j^{(NL)} - \epsilon_i^{(L)}$	F_{ij}
3	BD	C	15	O	18	BD*	N	63	H	64	1.55	0.99	0.035
	LP	O	18	-	-	BD*	N	63	H	64	2.65	1.32	0.053
	LP	O	18	-	-	BD*	N	63	H	64	0.64	0.87	0.022
	BD*	C	15	O	18	BD*	N	63	H	64	0.45	0.46	0.037
	BD	N	63	H	64	BD*	C	15	O	18	0.30	0.76	0.014
4	BD	O	3	H	4	RY*	O	44	-	-	0.14	1.95	0.015
	BD	O	3	H	4	RY*	O	44	-	-	0.28	2.52	0.024
	BD	O	3	H	4	BD*	C	41	O	44	0.45	1.51	0.023
	BD	O	3	H	4	BD*	C	41	O	44	0.26	0.92	0.015
	BD	C	41	O	44	BD*	O	3	H	4	0.42	1.64	0.024
	BD	C	41	O	44	BD*	O	3	H	4	0.60	0.96	0.022
	CR	O	44	-	-	BD*	O	3	H	4	0.27	19.85	0.066
	LP	O	44	-	-	BD*	O	3	H	4	20.42	1.27	0.144
	LP	O	44	-	-	BD*	O	3	H	4	2.09	0.84	0.038
	BD*	C	41	O	44	BD*	O	3	H	4	0.70	0.42	0.039
5	BD	C	8	N	11	BD*	O	55	H	56	0.41	1.25	0.021
	BD	N	11	H	12	BD*	O	55	H	56	0.41	1.16	0.020
	BD	N	11	H	13	BD*	O	55	H	56	1.84	1.15	0.042
	CR	N	11	-	-	BD*	O	55	H	56	0.53	15.02	0.081
	LP	N	11	-	-	BD*	O	55	H	56	41.64	0.86	0.169
	BD	O	55	H	56	RY*	N	11	-	-	0.05	1.66	0.008
	BD	O	55	H	56	RY*	N	11	-	-	0.06	1.50	0.009
	BD	O	55	H	56	BD*	C	8	N	11	0.07	1.22	0.008
	BD	O	55	H	56	BD*	N	11	H	12	0.13	1.32	0.012
6	BD	C	2	O	5	BD*	N	37	H	38	0.91	0.98	0.027
	LP	O	5	-	-	BD*	N	37	H	38	1.63	1.30	0.041
	LP	O	5	-	-	BD*	N	37	H	38	2.29	0.85	0.041
	BD*	C	2	O	5	BD*	N	37	H	38	0.21	0.43	0.024
	BD	N	37	H	38	BD*	C	2	O	5	0.11	0.77	0.009
7	BD	C	34	N	37	BD*	O	42	H	43	1.84	1.15	0.043
	BD	N	37	H	38	BD*	O	42	H	43	4.48	1.06	0.064
	BD	N	37	H	39	BD*	O	42	H	43	2.02	1.06	0.043
	CR	N	37	-	-	BD*	O	42	H	43	2.16	14.93	0.168
	LP	N	37	-	-	BD*	O	42	H	43	93.72	0.76	0.239
	BD	O	42	H	43	BD*	C	34	N	37	0.16	1.19	0.012
	BD	O	42	H	43	BD*	N	37	H	39	0.10	1.28	0.010
	BD*	O	42	H	43	RY*	N	37	-	-	0.06	1.66	0.031
	BD*	O	42	H	43	BD*	C	34	N	37	1.73	0.04	0.024
	BD*	O	42	H	43	BD*	N	37	H	39	0.21	0.13	0.015
8	BD	C	21	H	22	BD*	O	29	H	30	0.08	1.02	0.008
	BD	C	21	N	24	BD*	O	29	H	30	0.99	1.25	0.032
	BD	C	21	N	24	BD*	O	29	H	30	0.99	1.25	0.032
9	BD	N	24	H	25	BD*	O	29	H	30	1.28	1.16	0.035
	BD	N	24	H	26	BD*	O	29	H	30	0.27	1.16	0.016
	CR	N	24	-	-	BD*	O	29	H	30	0.58	15.03	0.085
	LP	N	24	-	-	BD*	O	29	H	30	42.86	0.86	0.172
	BD	O	29	H	30	RY*	N	24	-	-	0.11	1.83	0.013
	BD	O	29	H	30	BD*	N	24	H	26	0.22	1.31	0.015

References

[1] Cornell, W. D.; Cieplak, P.; Bayly, C. I.; Gould, I. R.; Merz, K. M. J.; Ferguson, D. M.; Spellmeyer, D. C.; Fox, T.; Caldwell, J. W.; Kollman, P. A. *Journal of the American Chemical Society* **1995**, *117*, 5179–5197.

[2] Weiner, P. K.; Kollman, P. A. *Journal of Computational Chemistry* **1981**, *2*, 287–303.

[3] Weiner, S.; Kollman, P.; Case, D.; Singh, U.; Ghio, C.; Alagona, G.; Profeta, S. J.; Weiner, P. *Journal of the American Chemical Society* **1984**, *106*, 765–784.

[4] Weiner, S. J.; Kollman, P. A.; Nguyen, D. T.; Case, D. A. *Journal of Computational Chemistry* **1986**, *7*, 230–252.

[5] Zhang, W.; Hou, T.; nad Wilson S. Ross, C. S.; Case, D. A. Leap and Gleap manual for AmberTools. 2008.

[6] Wang, J.; Wolf, R. M.; Caldwell, J. W.; Kollman, P. A.; Case, D. A. *Journal of Computational Chemistry* **2004**, *25*, 1157–1174.

[7] Cornell, W. D.; Cieplak, P.; Bayly, C. I.; Kollmann, P. A. *Journal of the American Chemical Society* **1993**, *115*, 9620–9631.

[8] Frisch, M. J. et al. Gaussian 09 Revision B.01. 2010.

[9] Berendsen, H. J. C.; Postma, J. P. M.; van Gunsteren, W. F.; DiNola, A.; Haak, J. R. *The Journal of Chemical Physics* **1984**, *81*, 3684.

[10] Andersen, H. C. *The Journal of Chemical Physics* **1980**, *72*, 2384–2393.

[11] Loncharich, R. J.; Brooks, B. R.; Pastor, R. W. *Biopolymers* **1992**, *32*, 523–535.

[12] Sanz, M. E.; Lesarri, A.; Peña, M. I.; Vaquero, V.; Cortijo, V.; López, J. C.; Alonso, J. L. *Journal of the American Chemical Society* **2006**, *128*, 3812–3817.

[13] Jeffrey, G. A. *An Introduction to Hydrogen Bonding (Topics in Physical Chemistry)*; Oxford University Press, 1997.